Supplementary information for

Photoacoustic-enabled automatic vascular navigation: accurate and naked-eye real-time visualization of deep-seated vessels

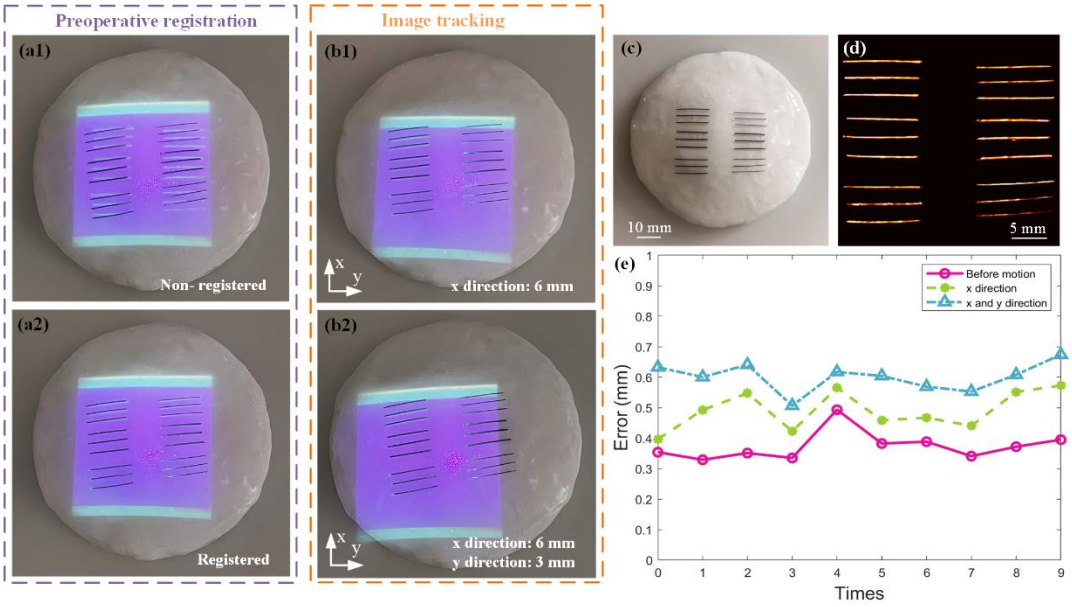

Fig. S1. The results of vascular localization accuracy verification on phantom experiments 2. (a1) The result of PA image was not registered with the phantom. (a2) The result of PA image was registered with phantom. (b1) The result of PA image reprojection after the phantom moved 6 mm in the x direction. (b2) The result of PA image reprojection after the phantom moved 6 mm in the x direction and 3 mm in the y direction. (c) Picture of the phantom sample. (d) 2D PA image of the phantom. (e) Projection error statistics of preoperative image registration and intraoperative image tracking quantified by repeating the experiment 10 times.

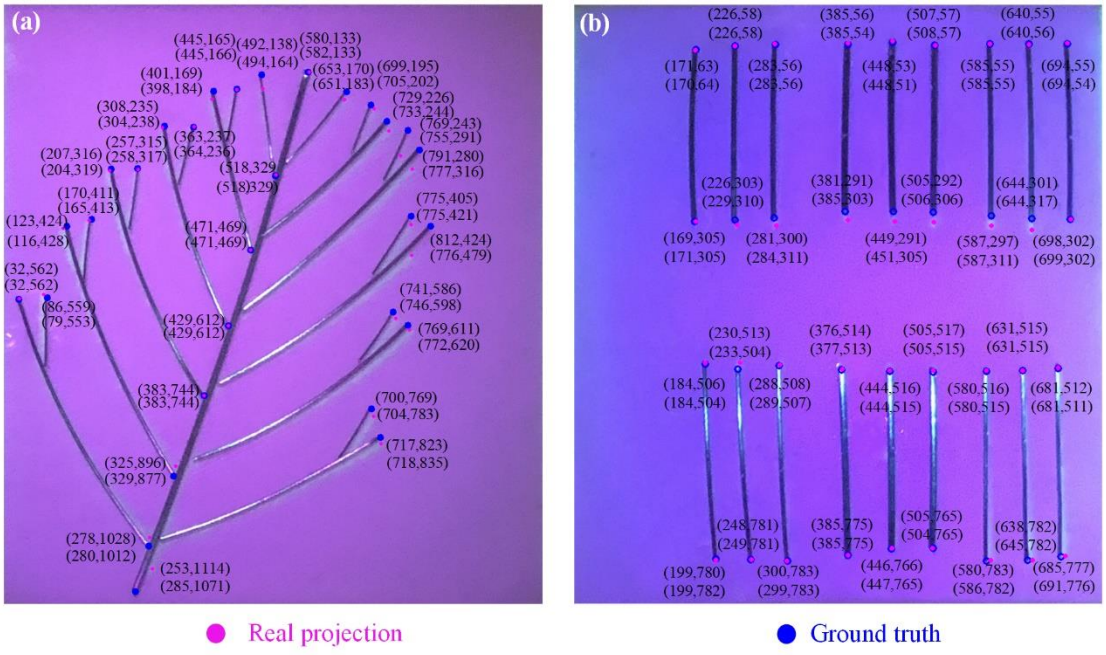

Fig. S2. Error calculation methods of phantom verification experiment 1 and experiment 2. The blue points were the points selected on the real phantom, and the pink points were the points selected on the actual projection. (a) The registered image in the phantom experiment 1, 30 edge points corresponding to the real phantom and the actual projection were selected to extract coordinates and calculate errors. The RMSE of experiment 1 is 17.34 pixels, and the spatial resolution is 0.039 mm per pixel (1029 × 1140 pixels for the projection area of ~40 × 45 mm), and the real error is ~0.676 mm. (b) The registered image in the phantom experiment 2, 36 endpoints corresponding to the real phantom and the actual projection were selected, coordinates were extracted to calculate the error using the root mean square error (RMSE), and finally converted into the real error. The RMSE of this result is about 6.35 pixels, and the spatial resolution is 0.055 mm per pixel (744 × 844 pixels for the projection area of ~41.1 × 46.6 mm), and the real error is ~0.349 mm.

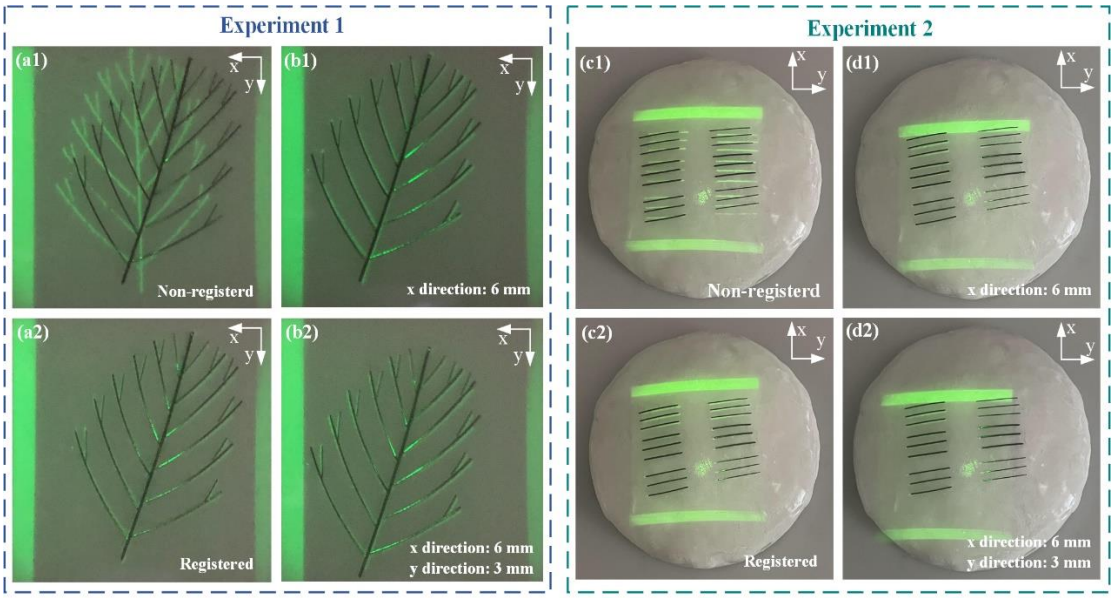

Fig. S3. The projection results on phantom experiments 1 and 2 after switching LED light source to green. (a1), (a2) Non-registered and Registered results during preoperative image registration in phantom experiment 1. (b1) Result of PA image reprojection after phantom 1 moved 6 mm in the x direction during the intraoperative image tracking process. (b2) Result of PA image reprojection after phantom 1 moved 6 mm in the x direction and 3 mm in the y direction during the intraoperative image tracking process. (c1), (c2) Non-registered and Registered results during preoperative image registration in phantom experiment 2. (d1) Result of PA image reprojection after phantom 2 moved 6 mm in the x direction during the intraoperative image tracking process. (d2) The reprojection result of PA image after phantom 2 moved 6 mm in the x direction and 3 mm in the y direction during the intraoperative image tracking process.

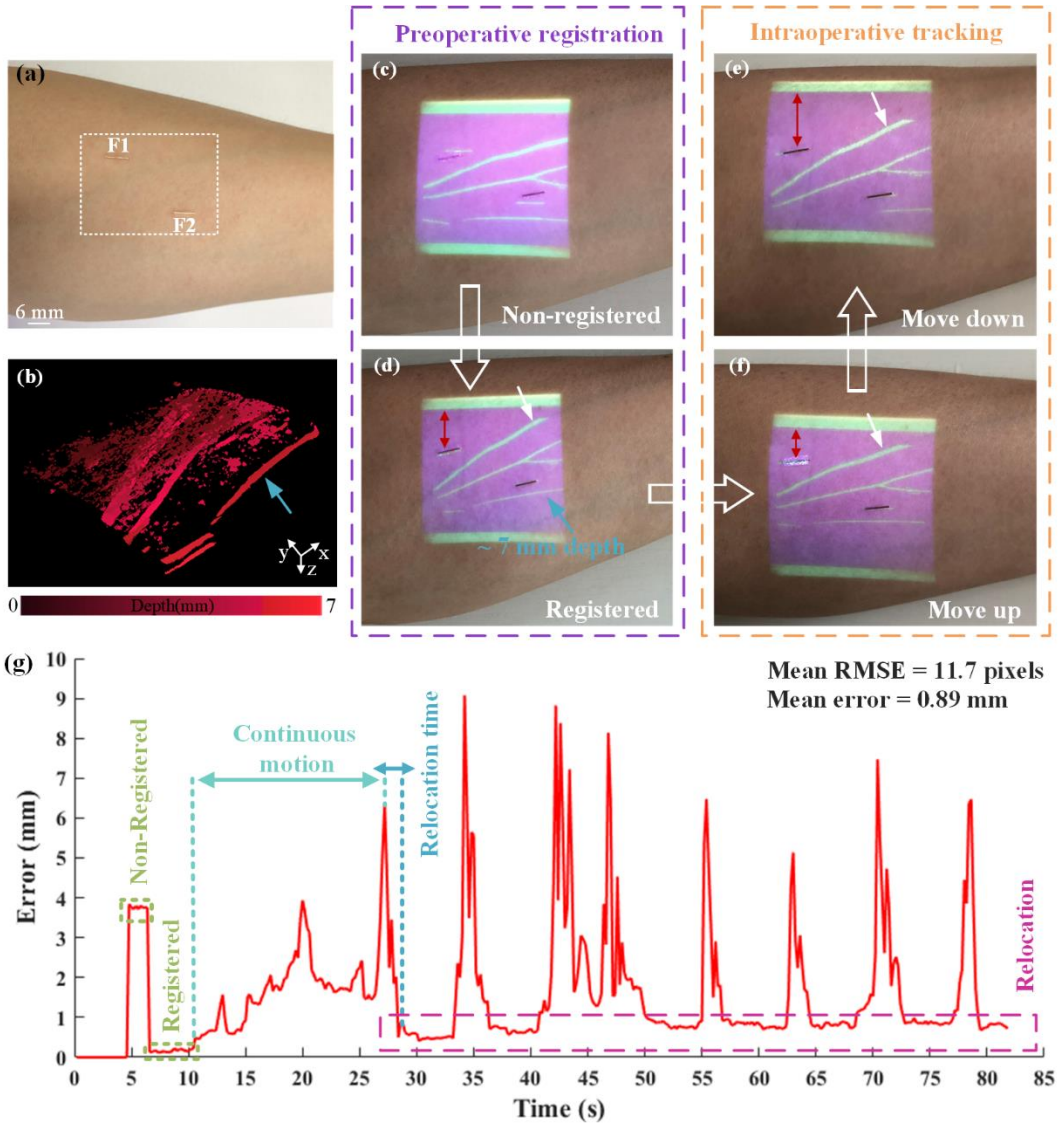

Fig. S4. (a) Picture of human arm. White dotted box was selected for PA imaging, F1 and F2 were two marks placed randomly. (b) 3D PA vascular image correspond to White dotted box. (c) Result of vascular image without registration on the surface. (d) Result of registered after 2D vascular image projected on the surgical surface with the white light source. (e) Result of image reprojection after moving down in (f). (f) Result of image reprojection after moving up during preoperative image registration. (g) Error statistics chart of the whole demonstration process based on the demonstration video of supplementary movie 4a on the human arm (supplementary movie 4a, MP4, 7.40 MB).

Application cases of automatic vascular navigation method

Application case 1: In injection microplastic surgery, fillers are usually injected in the dermis, however, it can happen that fillers are accidentally injected into the arterial vessels due to abnormal vascular anatomy, even by experienced surgeons, which can lead to devastating injuries such as blindness and stroke[47,48], while accurate preoperative mastering of the facial vascular network structure can avoid this situation. Using our proposed method, facial blood vessels can be accurately projected onto the skin surface in real time, providing vascular navigation for injectable fillers as a way to avoid medical errors. Therefore, we conducted the following experiment.

A 30 × 38 mm^2 area on the human face was selected for photoacoustic imaging, and the spot size was chosen to be 35 × 2 mm^2, the 1064 nm wavelength laser was also selected for excitation of the PA signals.

In addition, two carbon bars of 0.5 mm in diameter and 6 mm in length were placed randomly in the area for registration, as shown in Fig. S5(a). The reconstructed PA image after imaging is shown in Fig. S5(b). The structure of the blood vessels in the reconstructed PA image corresponds to the human facial vascular anatomy in Fig. S5(f). Using our proposed method, the obtained facial vascular image can be accurately projected at the corresponding locations to provide vascular navigation for intraoperative fillers injection, as shown in Fig. S5(c1). Once the blood vessels are accurately located, accurate injections can be performed, as shown in Fig. S5(c2), where we performed a simulated injection using a syringe.

Application case 2: In coronary intervention surgery, using the radial artery as the catheter entrance has the advantage of high success rate and few complications. It is a common practice to use the radial artery of the arm as the catheter entrance. According to the experiment described in the text, we selected an area of 30 × 38 mm2 on the human arm for PA imaging, and the reconstructed 2D photoacoustic blood vessel was shown in Fig. S5(d). As can be seen from the anatomical map of the arm blood vessels in Fig. S5(g), our reconstructed blood vessels were consistent with the anatomical structure. Fig. S4 showed that white light source was used to project blood vessels on the skin surface of the arm for accurate localization of deep blood vessels. In this experiment, green light source was used for projection, and different visual effects could be presented on the skin surface by changing the color of the light source, as shown in Fig. S5(e1) and (e2). With this automatic vascular navigation method, the radial artery can be quickly and accurately located, saving operation time and improving the success rate of surgery.
Therefore, the proposed automatic vascular navigation method is not unique in the application cases, and it is feasible in different organisms and different parts, which proves the great value and significance of our proposed method.

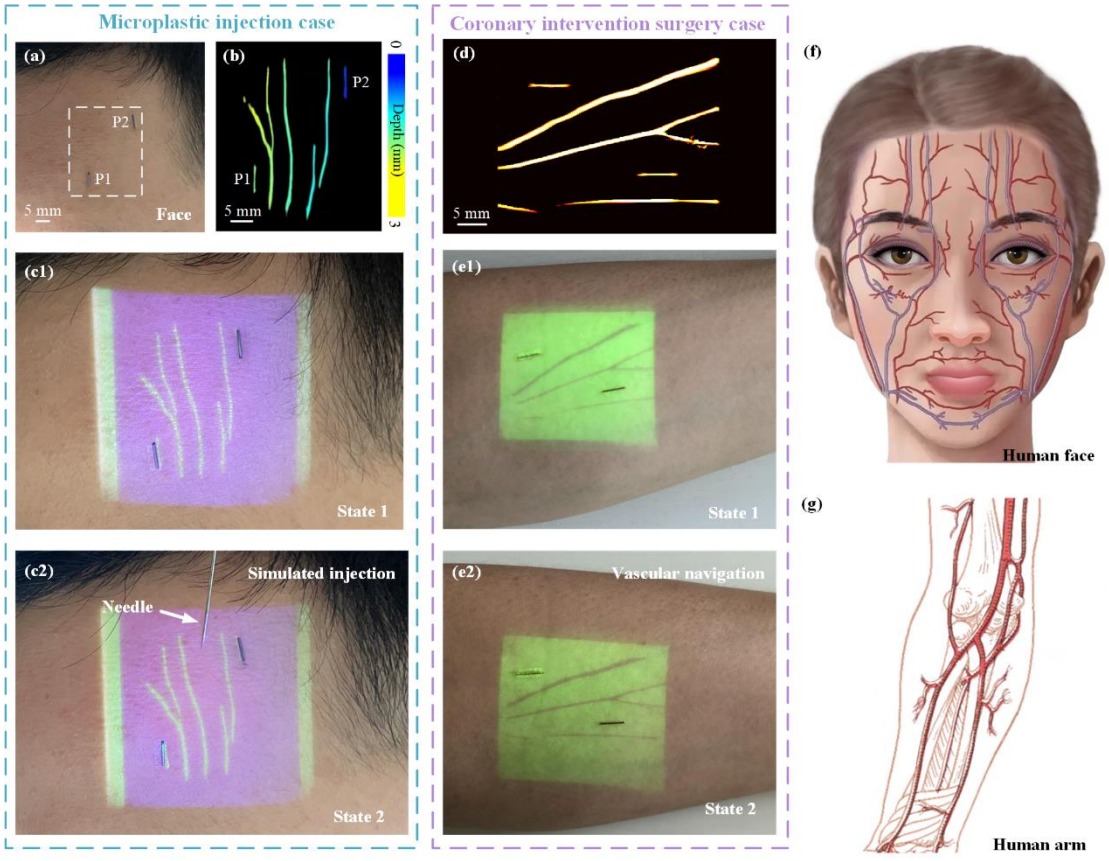

Fig. S5. (a) Picture of a human arm face. White dotted box was selected for PA imaging, F1 and F2 were two marks placed randomly. (b) 2D PA vascular images correspond to White dotted box. (c1) A state of registered after 2D vascular image projected on the surgical surface with the white light source. (c2) Simulated injection using automated vascular navigation methods. (d) 2D PA vascular image correspond to White dotted box of Fig. S4(a). (e1) A state of registered after 2D vascular image projected on the surgical surface with the green light source. (e1) Another state of registered after 2D vascular image projected on the surgical surface. (f) Anatomical structure of human facial blood vessels. (g) Anatomical structure of human arm blood vessels.

Information of the supplementary videos:

Supplementary Movie 1. The demonstration of vascular localization in phantom experiment 1, which is divided into preoperative image registration and intraoperative image tracking. The video demonstrates that PA images can be visualized on phantom surface in real time.

Supplementary Movie 2. The demonstration of real-time visualization of PA images on phantom surface in the phantom experiment 2, and demonstrated the specific steps of preoperative image registration and intraoperative image realization in detail.

Supplementary Movie 3. The demonstration of mixed reality on a rabbit's thigh. By projecting the PA vascular images directly on the rabbit's thigh surface, the deep blood vessels under the skin could be visualized directly by the naked eye in real time.

Supplementary Movie 4a. The demonstration of augmented reality on the human arm. The 3D vascular image and 3D surface model were fused to set up a PA vascular navigator in the 3D point cloud space, and the vascular navigator can be rotated and scaled in the 3D point cloud space.

Supplementary Movie 4b. The demonstration of mixed reality on the human arm. With the help of mixed reality, deep blood vessels can be directly visualized on the surface of human skin for rapid and accurate locating of blood vessels.